ADVANCED FUNCTIONAL MATERIALS

www.afm-journal.de

Hybrid Nanocomposites

On page 37, S.-W. Kim and co-workers report unidirectional high-power generation from piezoelectric nanogenerators via stress-induced dipole alignment from single-crystalline piezoelectric perovskite $ZnSnO_3$ nanocube/polydimethylsiloxane hybrids. This is achieved without applying electrical poling. A recordable large output voltage of about 20 V and an output current density of about 1 μA cm^{-2} from the device are successfully obtained while rolling under a vehicle tire.

Organic Photovoltaics

Exciton dissociation pathways within a polymer bulk heterojunction film in a solar cell device is investigated by L. Yu, L. X. Chen, and co-workers on page 10. The blue fullerene derivative PCBM acts as an electron acceptor and the yellow ribbons represent the investigated low-bandgap polymer PTB7. The polymer forms both ordered pi-stacked domains and disordered domains within the film. This image was created by Nanjia Zhou from Northwestern University.

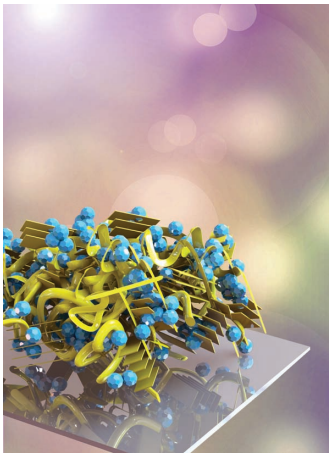

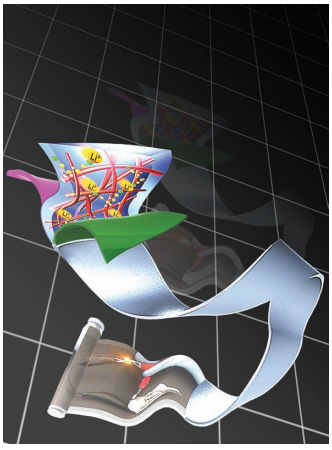

Flexible Batteries

Thin, deformable, and safety-reinforced plastic crystal polymer electrolytes for use in high-performance flexible lithium-ion batteries with aesthetic versatility and robust safety features is reported on page 44 by S.-Y. Lee and co-workers. The combination of a plastic crystal polymer electrolyte matrix with a compliant nonwoven skeleton enables the fabrication of the innovative polymer electrolyte with optimized attributes. The cell assembled with the polymer electrolyte exhibits stable electrochemical performance under severely deformed states (even a wrinkled state), without suffering from internal short-circuit failures.

CONTENTS

EDITORIAL

FEATURE ARTICLE

Organic Photovoltaics

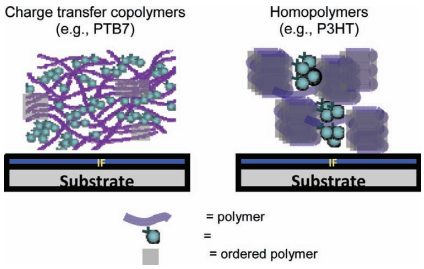

The excitonic dissociation pathways in the high-performance, low bandgap "in-chain donor-acceptor" polymer PTB7 are investigated by transient absorption spectroscopy and grazing incidence spectroscopy. The effects of the amplitude and kinetics of inter- and intramolecular charge transfer state spectra, along with a detailed morphology analysis, are investigated and compared to those of conventional semiconducting homopolymers.

FULL PAPERS

Organic Photovoltaics

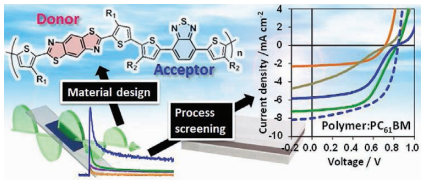

Benzobisthiazole (BBTz), commonly an acceptor unit in low-bandgap polymers of organic photovoltaics, is used as weak donor and polymerized with benzothiadiazole (BT). The BBTz-BT copolymers exhibit deep HOMO (–5.7 eV) and 3.8% power conversion efficiency in an inverted cell. Xe-flash time-resolved microwave conductivity is shown to be a versatile tool for decision-making on the molecular design strategy.

Hybrid Nanocomposites

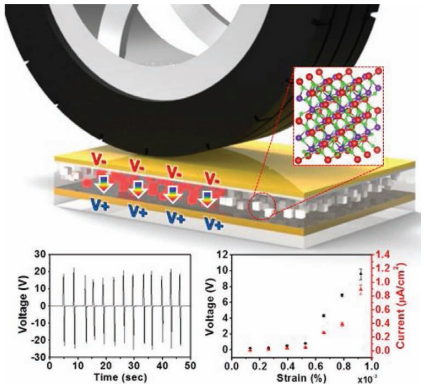

The unidirectional high-power generation via stress-induced dipole alignment from single-crystalline piezoelectric perovskite $ZnSnO_3$ nanocubes/polydimethylsiloxane hybrid piezoelectric nanogenerator without applying electrical poling is demonstrated. A recordable large output voltage of about 20 V and an output current density value of about 1 μA cm^{-2} from a single nanogenerator cell are successfully obtained under rolling of a vehicle tire.

FULL PAPERS

A new class of thin, deformable, and safety-reinforced plastic crystal polymer electrolytes is reported as an innovative solid electrolyte for use in high-performance flexible lithium-ion batteries with aesthetic versatility and robust safety features. The combination of plastic crystal polymer electrolyte matrix with a compliant nonwoven skeleton enables the fabrication of the polymer electrolytes with optimized attributes.

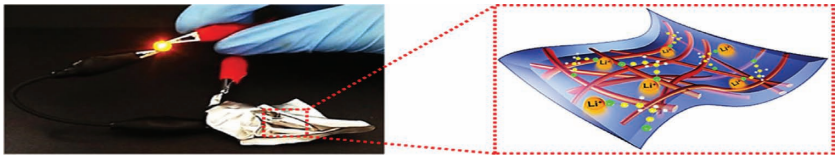

Flexible Batteries

A single layer, aqueous HgTe quantum dot (QD)-based photoconductor with fast temporal response is demonstrated. The device is fabricated using a simple spray-coating process and shows excellent stability in ambient conditions. The carrier mobility, the energy levels and carrier lifetimes associated with the trap states of the QDs are identified and correlated with the origin of the fast time response.

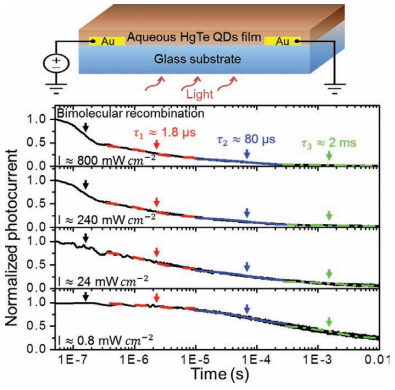

Photodetectors

Omniphobic fluoroalkylated ("R^F") paper, both hydrophobic and oleophobic, is formed by silanization of the cellulose fibers of paper with fluoroalkyl chains. R^F paper is highly permeable to gases and mechanically flexible, which allows it to be folded into functional shapes to form microtiter plates and liquid-filled gas sensors.

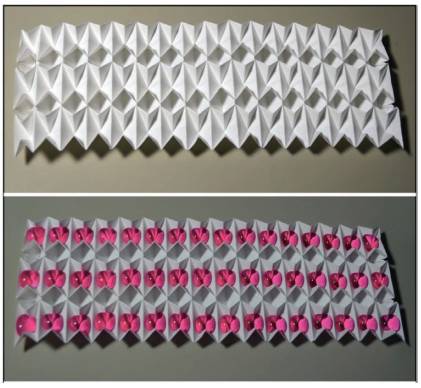

Omniphobicity

Understanding the chemical and magnetic properties of the interface in ferromagnetic/ferroelectric composites is key to achieving magneto-electric coupling. An irreversible oxidation can occur at the interface when applying an electric field. Basic material properties determine at which field magnitude and polarity the process may happen. These results are important for further development of artificial multiferroic systems.

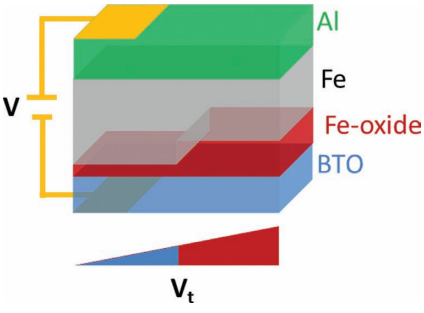

Ferroics

CONTENTS

FULL PAPERS

Carbon Nanotubes

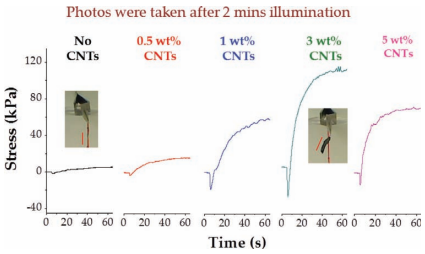

A composite is formed between a polymer that can generate anomalous photothermal contraction and few-walled carbon nanotubes. The new composite exhibits giant and reversible contraction in response to NIR stimulation. This significant enhancement enables the creation of high-performance near-IR-based actuators and efficient photothermal or thermal energy conversion.

Batteries

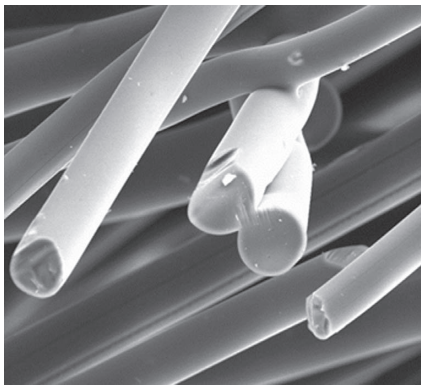

A novel synthetic technique for lignin-based carbon fibers, where the fibers are fused to each other resulting in monolithic fibrous mats, is described. The unique fiber microstructures and mat morphologies provide favorable electrochemical performance for lithium ion battery anode applications. The fibers cycle reversibly versus Li metal in alkyl carbonate electrolytes.

Hollow Spheres

Urchin-like mesoporous TiO_2 hollow spheres (UMTHS) are successfully prepared on a gram scale by a designed targeted-etching process. The key feature of the strategy is the etching reconstruction of amorphous hydrous TiO_2 solid spheres (ATHSS), creating a hollow interior and an urchin-like shell consisting of radially standing single-crystal anatase nanothorns with exposed {101} facets.

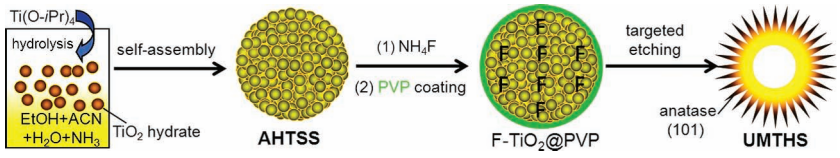

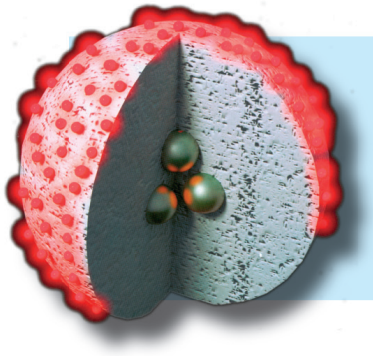

How to contact us:

Editorial Office:
Phone: (+49) 6201-606-286/531
Fax: (+49) 6201-606-500
Email: afm@wiley-vch.de

Reprints:
cherth@wiley-vch.de

Copyright Permission:
Fax: (+49) 6201-606-332
Email: rights@wiley-vch.de

FULL PAPERS

Vertically aligned silicon nanowire arrays with 55 nm diameter and 490 nm pitch are fabricated over large areas using a scalable and inexpensive bottom-up fabrication method (the combination of metal-assisted chemical etching and nanosphere lithography). These dimensions, typically fabricated with e-beam lithography, are achieved with large-scale reduction of nanospheres, a thin Au catalyst layer with Ti, and optimized etchant mixture.

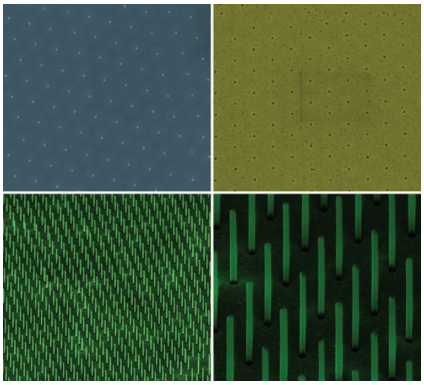

Nanowires

The novelty of the rGO FET strain sensor is the incorporation of an rGO channel as a sensing layer in which modulation of the inter-nanosheet resistance (R_{inter}) due to weak coupling between adjacent nanosheets induces a large change in the transconductance of the rGO FET. The rGO FET device is ultrasensitive to extremely low strain levels, as low as 0.02%.

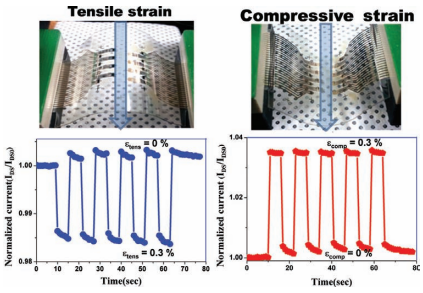

Sensors

A bottom-up approach is developed to build 3D architectures by 2D nanosheets such as MoS_2 and graphene oxide nanosheets as building blocks. The resulting 3D architectures possess favorable diffusion kinetics for both lithium and electrons, leading to excellent electrochemical performance. Such a simple and low-cost assembly protocol will provide a new pathway for the large-scale production of various functional 3D architectures for energy storage and conversions.

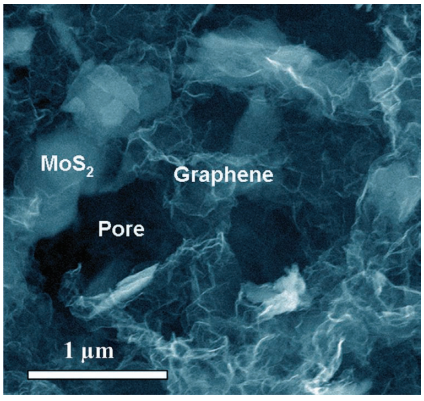

Nanosheets

Growth via attachment: Ultrathin Pd nanowires are synthesized by controlling the reaction kinetics and thus the nucleation and growth of Pd nanoparticles, as well as their coalescence into chain-like nanostructures. The Pd nanowires show a catalytic activity 2.5 times higher than the conventional Pd/C catalyst towards formic acid oxidation.

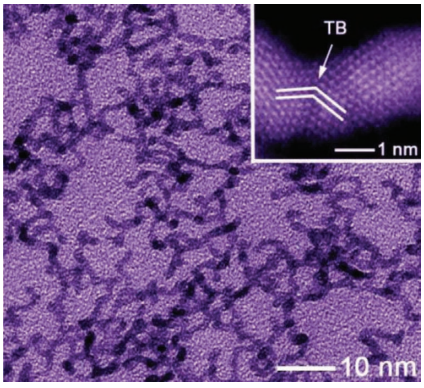

Nanowires

CONTENTS

FULL PAPERS

Organic Photovoltaics

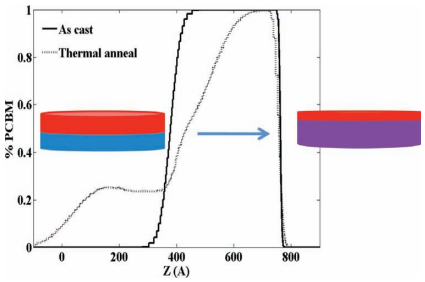

Fullerene diffuses into low-bandgap polymers with thermal annealing. Polymer/fullerene mixing is found to be crucial for optimal device performance.

Solar Cells

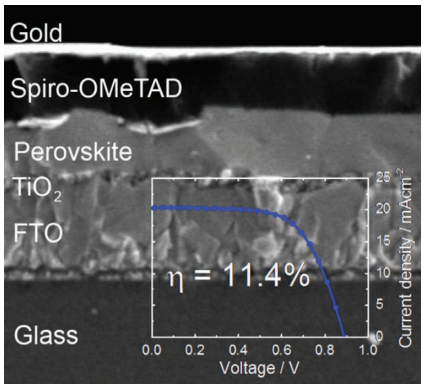

The critical role of perovskite morphology in planar heterojunction perovskite solar cells is probed and understood. Dewetting of perovskite films is minimized, to achieve uniform 100% coverage perovskite layers. Solution cast planar heterojunction solar cells with efficiencies of up to 11.4% are fabricated, a new record for such cells with no mesoporous layer.

Polymer Solar Cells

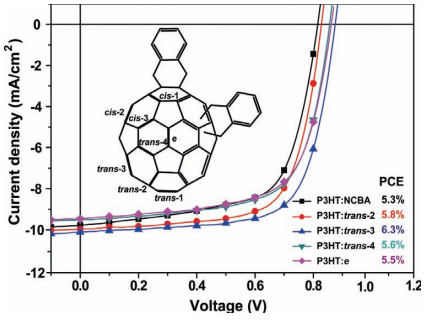

The *trans*-2, *trans*-3, *trans*-4, and *e* isomers of dihydronaphthyl-based [60] fullerene bisadduct (NCBA) are isolated and used as acceptors for P3HT-based polymer solar cells (PSCs), and the corresponding PSCs fabricated by the four isomers show power conversion efficiencies of 5.8, 6.3, 5.6, and 5.5%, respectively, which are higher than that based on an NCBA mixture (5.3%), suggesting the necessity to use the individual fullerene bisadduct isomer for high-performance PSCs.

Nanocrystals

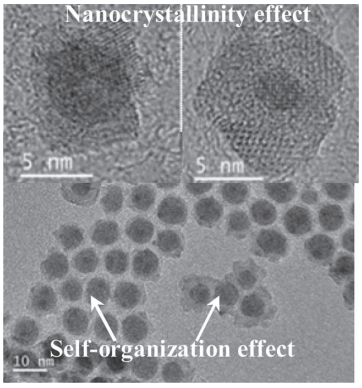

Both the nanocrystallinity of Co nanoparticles (NPs) and their 2D hexagonal organization are for the first time shown to have a significant impact on the oxidation process rate, enabling various nanostructures, such as core-shell NPs, to be obtained. The Co core is either polycrystalline or hexagonal close-packed (hcp) single-crystalline, whereas the oxide shell is composed either of monoxide CoO or of a Co_3O_4 spinel.